Supporting Information

Optical Control of Calcium Affinity in a Spiroamido-rhodamine Based Calcium Chelator

Liangxing Wu, Yingrui Dai and Gerard Marriott*

Department of Bioengineering, University of California-Berkeley, Berkeley, CA 94720

marriott1@berkeley.edu

Synthetic Materials and Methods: All reactions were carried out under an atmosphere of dry nitrogen. Glasswares were oven-dried prior to use. Unless otherwise indicated, common reagents or materials were obtained from commercial source and used without further purification. Dry distilled THF and CH_2Cl_2 were obtained from Acros and used as received. Flash column chromatography was performed using silica gel 60 (70-230 mesh). Analytical thin layer chromatography (TLC) was carried out on Merck silica gel plates with QF-254 indicator and visualized by UV. ^1H and ^{13}C NMR spectra were recorded at room temperature on a Bruker 400 (400 MHz ^1H; 100 MHz ^{13}C) spectrometer at College of Chemistry NMR Facility at University of California, Berkeley. Chemical shifts were reported in ppm relative to the residual solvent signal ($CDCl_3$: 99.8 % D contains 0.05% v/v TMS, δ 7.26 ppm ^1H, δ 77.00 ppm ^{13}C; D_2O, δ 4.80 ppm ^1H). High-resolution mass spectral analyses were carried out at QB3/CCHEM Mass Spectrometry Facility at University of California, Berkeley.

Scheme S1. Synthesis of chelator **1**.

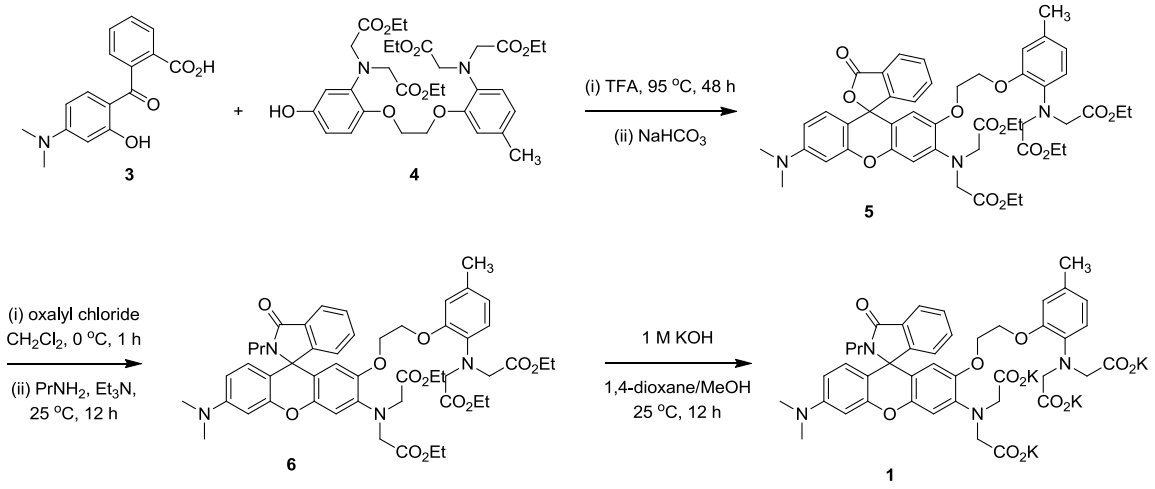

Synthesis of Compound 5: A 100 mL heavy wall pressure tube was charged with compound **3**[1] (342 mg, 1.2 mmol) and compound **4**[2] (619 mg, 1.0 mmol) then 10 mL TFA was added. The tube was sealed

[1] Liu, Q.-H.; Yan, X.-L.; Guo, J.-C.; Wang, D.-H.; Li, L.; Yan, F.-Y.; Chen, L.-G. *Spectrochim. Acta, Part A* **2009**, *73A*, 789-793.

[2] Grynkiewicz, G.; Poenie, M.; Tsien, R. Y. *J. Biol. Chem.* **1985**, *260*, 3440-3450.

and the reaction mixture was stirred at 95 ^{o}C for 48 h. After cooled to room temperature, the solution was concentrated under reduced pressure. The residue was dissolved in EtOAc and washed with saturated $NaHCO_3$ aqueous solution. The organic layer was then washed with water, brine and dried over Na_2SO_4. The solvents were removed in vacuo and the residue was purified by flash chromatography (60 % to 100 % EtOAc/Hexanes) to afford the product **5** as a pink solid (515 mg, 59 %). ^{1}H NMR (400 MHz, $CDCl_3$) δ 8.01 – 7.96 (m, 1H), 7.65 – 7.54 (m, 2H), 7.14 – 7.09 (m, 1H), 6.70 (d, *J* = 8.0 Hz, 1H), 6.67 – 6.61 (m, 2H), 6.59 – 6.55 (m, 2H), 6.45 (d, *J* = 2.5 Hz, 1H), 6.38 (dd, *J* = 8.9, 2.6 Hz, 1H), 6.12 (s, 1H), 4.18 (s, 4H), 4.13 – 3.85 (m, 16H), 2.97 (s, 6H), 2.23 (s, 3H), 1.18 – 1.10 (m, 12H); ^{13}C NMR (100 MHz, $CDCl_3$) δ 171.44, 170.98, 169.54, 153.16, 152.62, 151.94, 150.11, 146.76, 146.28, 141.99, 136.81, 134.71, 131.91, 129.51, 128.54, 126.96, 124.87, 123.77, 121.73, 119.12, 114.23, 111.37, 110.84, 108.70, 106.13, 105.88, 98.37, 84.44, 67.73, 66.78, 60.92, 60.55, 53.49, 53.45, 40.19, 20.86, 14.05, 13.98; HRMS (ESI) m/z calculated for $C_{47}H_{54}N_3O_{13}$ ($[M+H]^+$) 868.3651; found 868.3639.

Synthesis of Compound 6: Compound **5** (7 mg, 8 μmol) was dissolved in 0.3 mL CH_2Cl_2 and 10 μL DMF was added at 0 ^{o}C followed by oxalyl chloride (2 M in CH_2Cl_2, 20 μL). The red solution was stirred at 0 ^{o}C for 1 h then propylamine (33 μL, 0.4 mmol) and Et_3N (56 μL, 0.4 mmol) were added. The resulting colorless solution was stirred at room temperature overnight then diluted with 2 mL CH_2Cl_2. The solution was washed with water, brine then dried over Na_2SO_4. The solvent was removed under reduced pressure and the residue was purified by preparative TLC (20 % EtOAc/hexanes) to afford compound **6** (5 mg, 68 %) as a white solid. ^{1}H NMR (400 MHz, $CDCl_3$) δ 7.93 – 7.87 (m, 1H), 7.47 – 7.37 (m, 2H), 6.99 – 6.93 (m, 1H), 6.69 (d, *J* = 8.0 Hz, 1H), 6.66 – 6.61 (m, 1H), 6.59 – 6.53 (m, 2H), 6.46 (d, *J* = 8.8 Hz, 1H), 6.39 (d, *J* = 2.5 Hz, 1H), 6.36 – 6.30 (m, 1H), 4.26 – 3.80 (m, 20H), 3.10 – 3.00 (m, 2H), 2.96 (s, 6H), 2.23 (s, 3H), 1.23 – 1.04 (m, 14H), 0.68 (t, *J* = 7.4 Hz, 3H); ^{13}C NMR (100 MHz, $CDCl_3$) δ 171.46, 171.20, 168.07, 153.27, 152.71, 151.24, 150.13, 146.64, 146.37, 140.92, 136.79, 132.28, 131.91, 130.91, 128.69, 128.30, 123.37, 122.96, 121.71, 119.14, 114.10, 111.25, 110.51, 108.73, 106.09, 106.02, 98.47, 67.42, 66.75, 64.78, 60.95, 60.50, 53.49, 53.36, 42.24, 40.23, 21.74, 20.88, 14.07, 13.96, 11.79; HRMS (ESI) m/z calculated for $C_{50}H_{61}N_4O_{12}$ ($[M+H]^+$) 909.4280; found 909.4265.

Synthesis of Compound 1: Compound **6** (4 mg, 4.4 μmol) was dissolved in 0.3 mL 1,4-dioxane and 0.2 mL MeOH then KOH (44 μL, 1 M in H_2O) was added. The reaction mixture was stirred at room temperature in the dark for overnight. The solvents were removed under a nitrogen stream. The residue was purified by reverse phase column (Supel clean^{TM} LC-18 SPE, H_2O to 50 % MeOH/H_2O) to afford the product **1** (4 mg, 96 %) as a white solid. ^{1}H NMR (400 MHz, D_2O) δ 7.90 – 7.83 (m, 1H), 7.61 – 7.52 (m, 2H), 7.13 – 7.07 (m, 1H), 6.81 – 6.71 (m, 3H), 6.63 (s, 1H), 6.56 (dd, *J* = 9.2, 2.4 Hz, 1H), 6.47 (d, *J* = 8.8 Hz, 1H), 6.10 (s, 1H), 4.22 – 4.12 (m, 2H), 4.12 – 4.00 (m, 2H), 3.97 – 3.81 (m, 4H), 3.73 – 3.59 (m, 4H), 3.17 – 2.96 (m, 2H), 2.90 (s, 6H), 2.24 (s, 3H), 1.17 – 0.97 (m, 2H), 0.63 (t, *J* = 7.4 Hz, 3H); HRMS (ESI) m/z calculated for $C_{42}H_{43}N_4O_{12}$ ($[M-4K+3H]^-$) 795.2883; found 795.2876.

Scheme S2. Synthesis of model compound **2**.

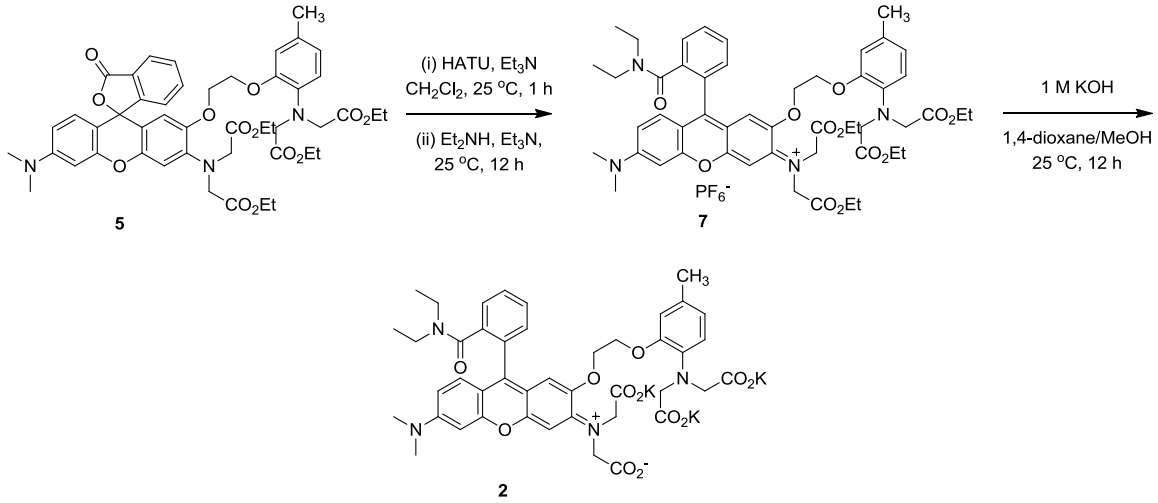

Synthesis of Compound 7: Compound **5** (26 mg, 0.03 mmol) was dissolved in 1.0 mL CH_2Cl_2 then HATU (23 mg, 0.06 mmol) and Et_3N (21 μL, 0.15 mmol) were added. The mixture was stirred at room temperature for 1 h and Et_2NH (16 μL, 0.15 mmol) was added. After stirring at room temperature overnight, the reaction mixture was diluted with CH_2Cl_2 then washed with water and brine. The organic layer was dried over Na_2SO_4 and the solvent was removed under reduced pressure. The residue was purified by preparative TLC (10 % MeOH/CH_2Cl_2) to afford the product **7** (34 mg, 97 %) as a red solid. ^{1}H NMR (400 MHz, $CDCl_3$) δ 7.72 – 7.63 (m, 2H), 7.58 – 7.51 (m, 1H), 7.38 – 7.29 (m, 2H), 7.21 – 7.15 (m, 1H), 6.84 (d, *J* = 2.4 Hz, 1H), 6.82 (s, 1H), 6.77 (d, *J* = 8.1 Hz, 1H), 6.73 (s, 1H), 6.71 – 6.66 (m, 1H), 6.62 – 6.58 (m, 1H), 4.50 – 4.29 (m, 4H), 4.19 – 3.99 (m, 16H), 3.35 (s, 6H), 3.33 – 3.12 (m, 2H), 3.06 – 2.92 (m, 2H), 2.24 (s, 3H), 1.20 – 1.13 (m, 12H), 1.05 (t, *J* = 7.0 Hz, 3H), 0.57 (t, *J* = 7.0 Hz, 3H); ^{13}C NMR (100 MHz, $CDCl_3$) δ 171.30, 169.23, 167.77, 157.73, 157.60, 156.22, 152.93, 150.40, 150.08, 147.87, 136.85, 136.76, 132.43, 131.30, 130.46, 129.71, 129.64, 129.54, 126.88, 122.19, 119.76, 116.32, 115.57, 115.39, 114.66, 109.86, 101.83, 96.20, 68.24, 66.44, 61.88, 60.59, 55.01, 53.55, 43.42, 41.12, 38.46, 20.87, 14.11, 13.91, 11.74; HRMS (ESI) m/z calculated for $C_{51}H_{63}N_4O_{12}$ ($[M\text{-}PF_6]^+$) 923.4437; found 923.4444.

Synthesis of Compound 2: Compound **7** (10 mg, 10 μmol) was dissolved in 0.5 mL 1,4-dioxane and 0.5 mL MeOH then KOH (100 μL, 1 M in H_2O) was added. The reaction mixture was stirred at room temperature in the dark for overnight. Reverse phase TLC indicated the reaction was complete. The excess KOH was neutralized by HCl (50 μL, 1 M in H_2O). The solvents were removed under a nitrogen stream. The residue was purified by reverse phase column (Supel clean^{TM} LC-18 SPE, H_2O to 50 % MeOH/H_2O) to afford the product **2** (8 mg, 92 %) as a red solid. ^{1}H NMR (400 MHz, D_2O) δ 7.75 – 7.63 (m, 2H), 7.62 – 7.55 (m, 1H), 7.54 – 7.48 (m, 1H), 7.20 – 7.08 (m, 2H), 7.00 – 6.93 (m, 1H), 6.93 – 6.85 (m, 2H), 6.84 – 6.77 (m, 1H), 6.77 – 6.72 (m, 1H), 6.69 – 6.63 (m, 1H), 4.47 – 4.10 (m, 8H), 3.98 (s, 4H), 3.25 – 2.88 (m, 10H), 2.30 (s, 3H), 0.95 (t, *J* = 6.8 Hz, 3H), 0.35 (t, *J* = 6.8 Hz, 3H); HRMS (ESI) m/z calculated for $C_{43}H_{47}N_4O_{12}$ ($[M\text{-}3K\text{+}4H]^+$) 811.3185; found 811.3199.

Spectroscopic Materials and Methods: Absorbance spectra were recorded on a Shimadzu UV-1601PC spectrophotometer at room temperature. Fluorescence spectra were obtained at room temperature on a AMINCO-Bowman Series 2 spectrofluorometer. Excitation and emission slits were set to 4 nm width. Millipore water was used to prepare all aqueous solutions. All spectroscopic measurements were performed at 20 ^{o}C.

Calcium Affinities: To determine the Ca^{2+} binding affinities for chelators **1** and **2**, the absorbance or fluorescence spectra of **1** and **2** were monitored in a series of calibration buffer containing various $[Ca^{2+}]_{free}$. The titration were repeated three times and the data were analyzed by a Hill plot: a plot of log $[(A - A_{min})/(A_{max} - A)] \equiv y$ versus log $[Ca^{2+}]_{free} \equiv x$, where A_{min} is the absorbance or fluorescence of the free chelator, A_{max} is the absorbance or fluorescence of the Ca^{2+} complex, and A is the absorbance or fluorescence at an intermediate Ca^{2+} level, all measured at the same wavelength. The slope of the Hill plot indicates the stoichiometry of the metal complex. The *x* intercept gives the log dissociation constant, log K_d of the complex.

At low μM $[Ca^{2+}]$, the free calcium concentration $[Ca^{2+}]_{free}$ were controlled by Ca-EGTA buffers, assuming an apparent dissociation constant for Ca-EGTA of 150.5 nM at pH 7.20. A series of calibration buffer containing various $[Ca^{2+}]_{free}$ was prepared by mixing two solutions[2, 3] from Biotium (*solution A*: 10 mM K_2EGTA, 100 mM KCl and 10 mM MOPS, pH 7.20; *solution B*: 10 mM CaEGTA, 100 mM KCl and 10 mM MOPS, pH 7.20). At higher $[Ca^{2+}]_{free}$ levels (> 10 μM), the calcium concentration was not buffered and $[Ca^{2+}]$ was adjusted by $CaCl_2$ in 10 mM MOPS, 100 mM KCl, pH 7.20.

(**a**) (**b**)

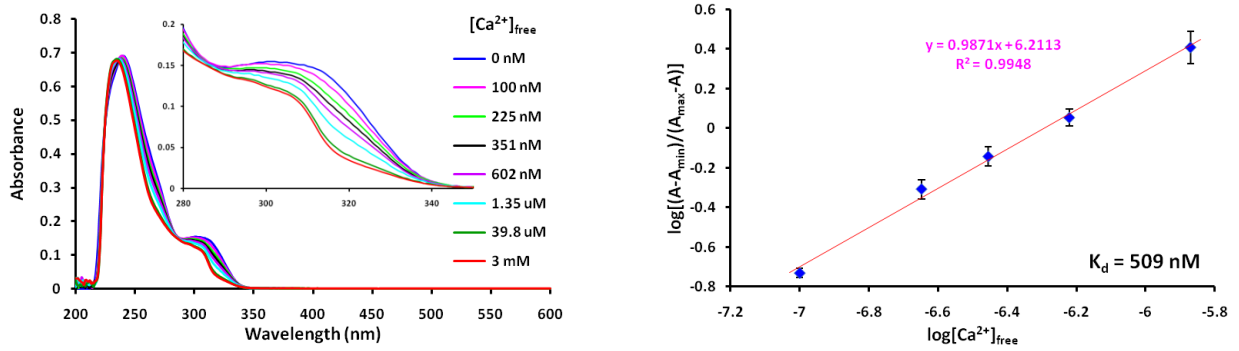

Figure S1. (**a**) Absorption spectra of compound **1** (20 μM) as a function of free Ca^{2+} concentration buffered with EGTA. After the free Ca^{2+} concentration was reached to 39.8 μM, addition of 3 mM $CaCl_2$ to the solution had little effect on the spectrum. Spectra were acquired in 10 mM MOPS, 100 mM KCl, pH 7.20; (**b**) Hill plot of the absorbance measured at 320 nm.

[3] Tsien, R. Y. *Biochemistry*, **1980**, *19*, 2396-2404

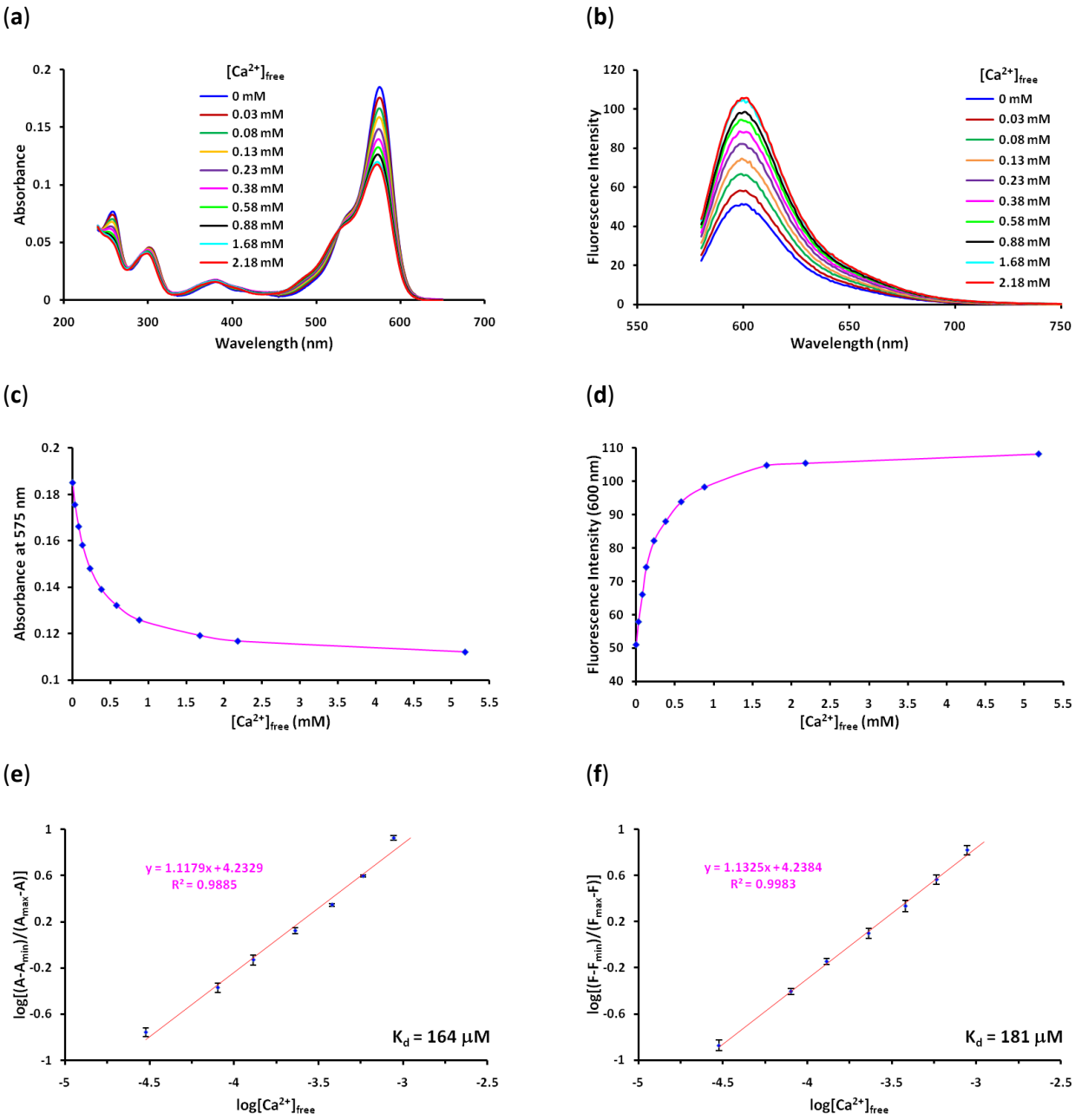

Figure S2. (**a**) Absorption and (**b**) fluorescence spectra of compound **2** (2 μM) as a function of free Ca^{2+} concentration adjusted by $CaCl_2$. After the Ca^{2+} concentration was reached to 1.68 mM, further addition of $CaCl_2$ had little effect on the spectrum. Spectra were acquired in 10 mM MOPS, 100 mM KCl, pH 7.20; (**c**) absorbance at 575 nm and (**d**) fluorescence intensities at 600 nm as a function of [Ca^{2+}]; (**e**) Hill plot of the absorbance measured at 575 nm; (**e**) Hill plot of the fluorescence intensity measured at 600 nm.

Magnesium Affinities: The Mg^{2+} binding affinities for the chelators were determined similarly as described for Ca^{2+}. Free [Mg^{2+}] was controlled by Mg^{2+}-EGTA buffer assuming an apparent dissociation constant for Mg^{2+}-EGTA complex of 19.73 mM at pH 7.20 in 10 mM MOPS, 0.1 M ionic strength at 20 ^{o}C. A series of calibration buffers containing various $[Mg^{2+}]_{free}$ were prepared by mixing two solutions (*solution A*: 1 mM EGTA, 100 mM KCl and 10 mM MOPS, pH 7.20; *solution B*: 6.1 mM EGTA, 105.1 mM $MgCl_2$ and 10 mM MOPS, pH 7.20) according to the methods developed by Tsien *et al*.[2] The buffer was prepared such that all solutions have 1 mM free H_2EGTA^{2-}. The free EGTA was needed to sequester the effect of Ca^{2+} contaminated in the $MgCl_2$.

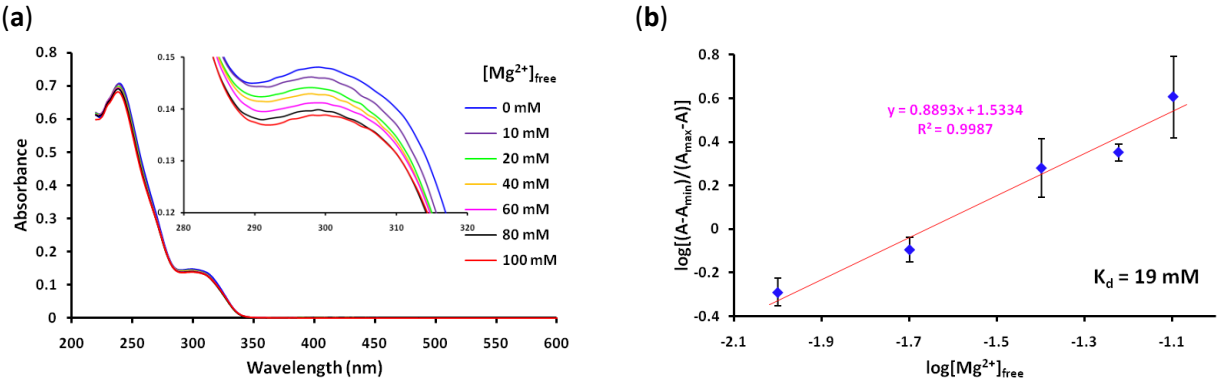

Figure S3. (**a**) Absorption spectra of compound **1** (20 μM) as a function of free Mg^{2+} concentration in 10 mM MOPS, pH 7.20; (**b**) Hill plot of the absorbance measured at 300 nm.

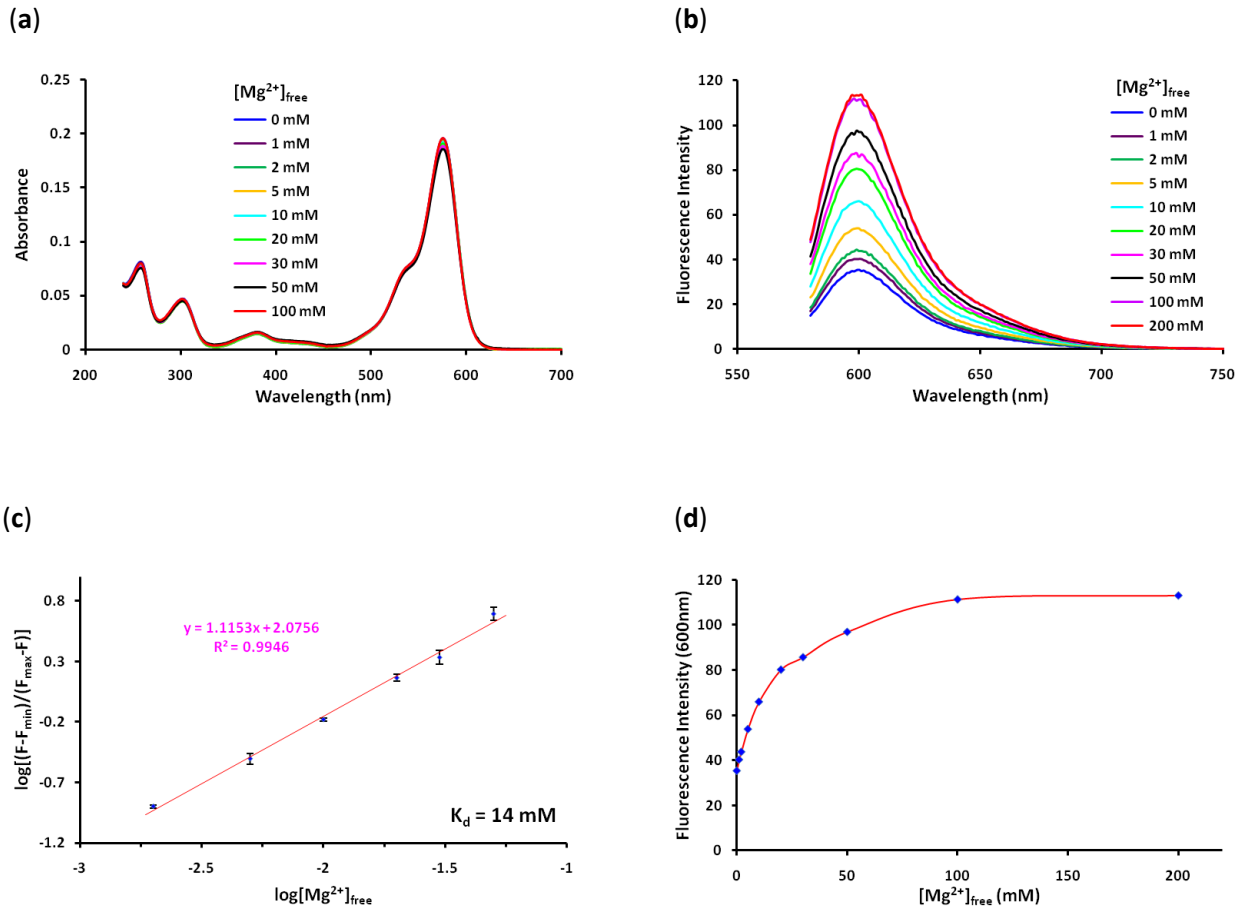

Figure S4. (**a**) Absorption spectra and (**b**) emission spectra of compound **2** (2 μM) as a function of free Mg^{2+} concentration in 10 mM MOPS, pH 7.20. After the Mg^{2+} concentration was reached to 100 mM, further addition of $MgCl_2$ had little effect on the spectrum; (**c**) Hill plot of the emission measured at 600 nm; (**d**) fluorescence intensities at 600 nm as a function of [Mg^{2+}].

Photochemical Materials and Methods: Opto-thermal switching of compound **1** (20 μM) was carried out in aqueous buffer (10 mM MOPS, 100 mM KCl, 1 mg/mL BSA, pH 7.20) at 20 ^{o}C in a quartz cuvette. Transilluminator (Stratagene 2040EV) was used as the 312 nm UV light source. The absorbance spectrum of the solution was recorded right before and after the solution was irradiated for 30 s with 312 nm UV light. Thermal ring-closure was examined by continuously monitoring the absorbance at 575 nm in the dark at 20 ^{o}C. Once all the open form was converted to the closed state, the solution was irradiated with 312 nm UV light for 30 s again and the above process was repeated several times. The switching process of **1** in the presence of excess Ca^{2+} or Mg^{2+} was examined similarly.

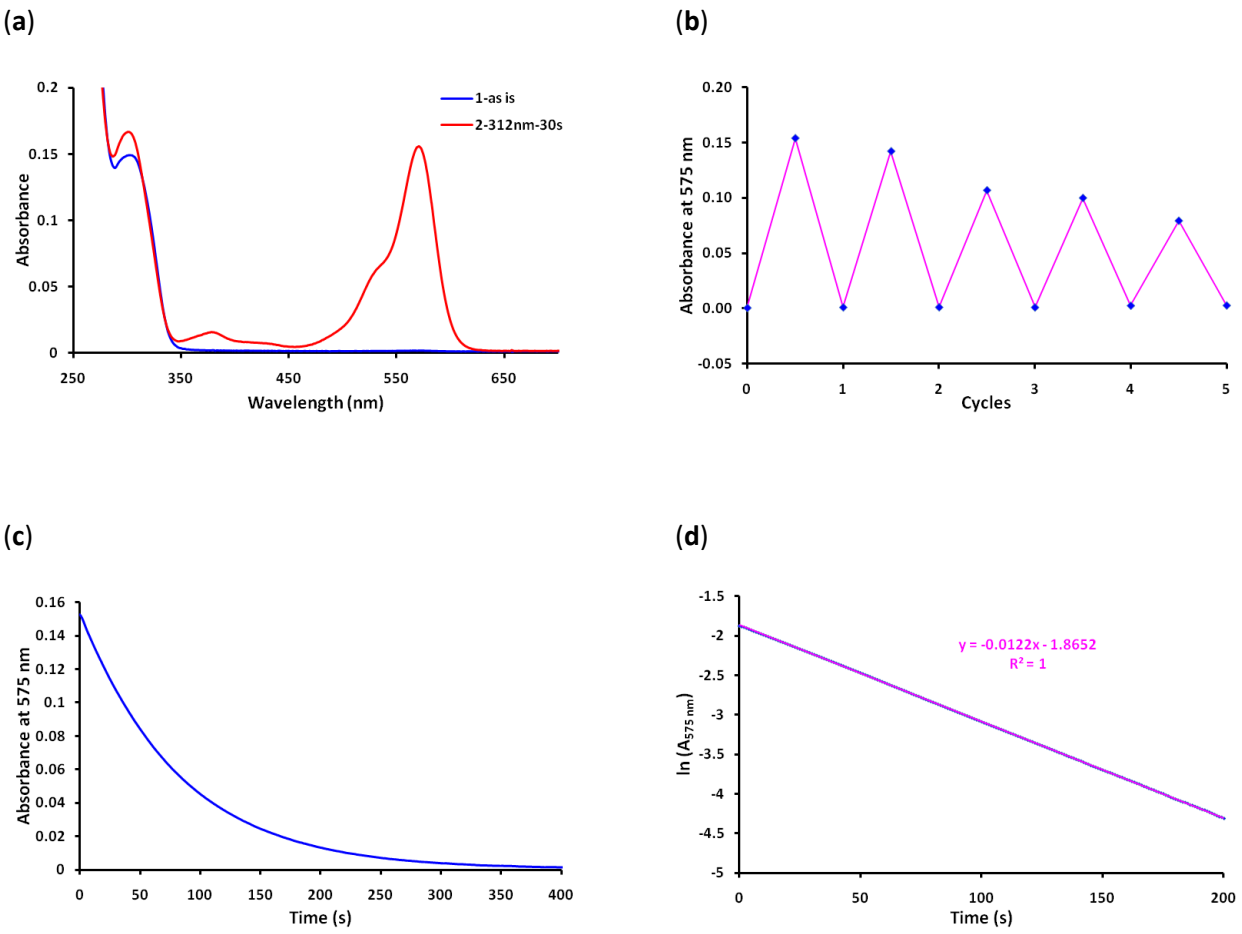

Figure S5. (**a**) Absorbance spectra of **1** (20 μM) as dissolved in a buffer solution (10 mM MOPS, 100 mM KCl, 1 mg/mL BSA, pH 7.20) and after irradiation with 312 nm light for 30 s; (**b**) absorbance changes at 575 nm of **1** in five cycles of UV irradiation (312 nm, 30 s) followed by thermal ring-closure in the dark; (**c**) time course for thermal ring-closure of **1** in the dark at 20 ^{o}C; (**d**) first-order rate plot for the thermal ring-closure of **1**.

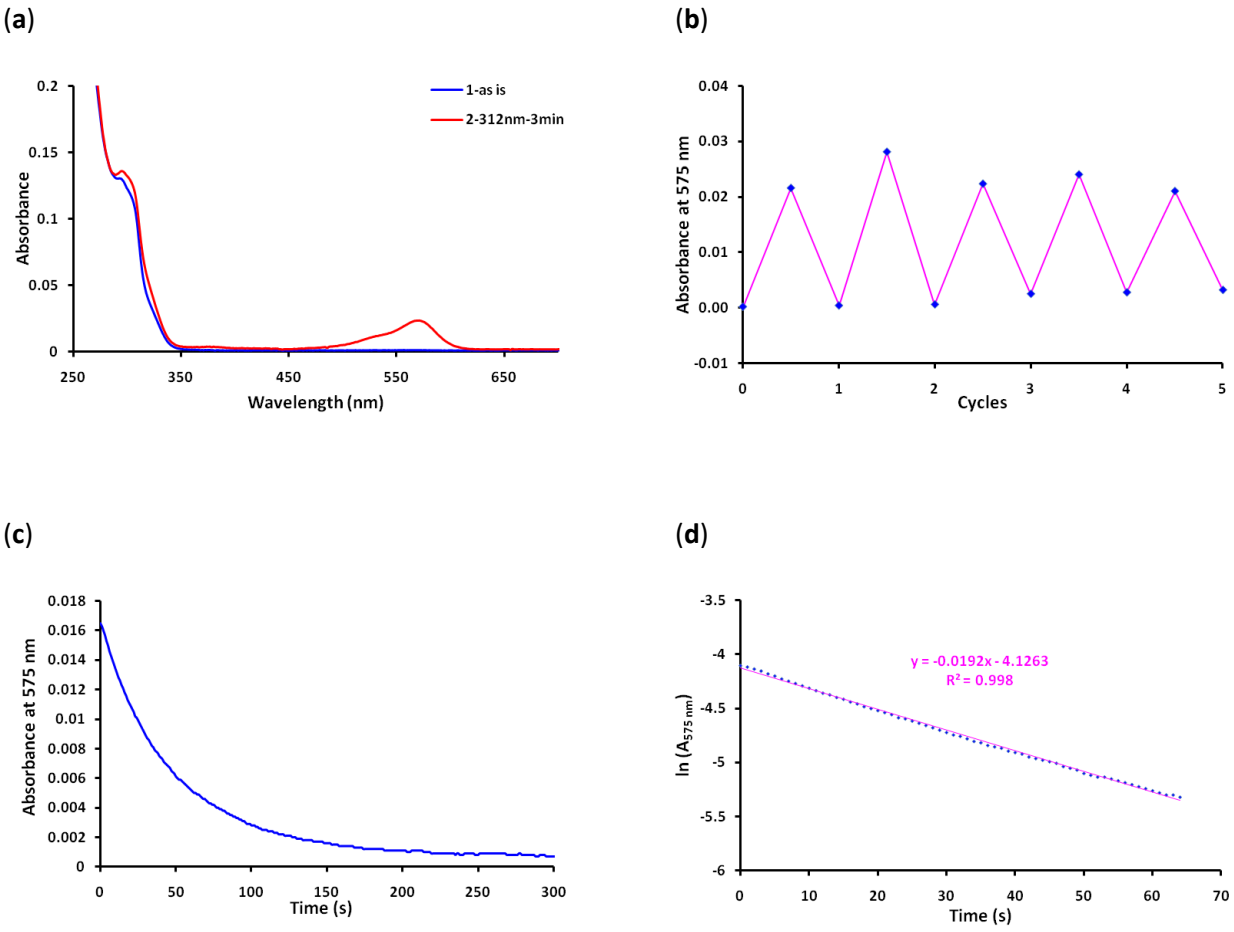

Figure S6. Opto-thermal switching properties of **1** (20 μM in 10 mM MOPS, 100 mM KCl, 1 mg/mL BSA, pH 7.2) in the presence of 100 μM Ca^{2+}: (**a**) absorbance spectra as dissolved in buffer solution and after irradiation with 312 nm light for 3 min; (**b**) absorbance changes at 575 nm in five cycles of UV irradiation (312 nm, 3 min) followed by thermal ring-closure in the dark; (**c**) time course for thermal ring-closure in the dark at 20 ^{o}C; (**d**) first-order rate plot for the thermal ring-closure.

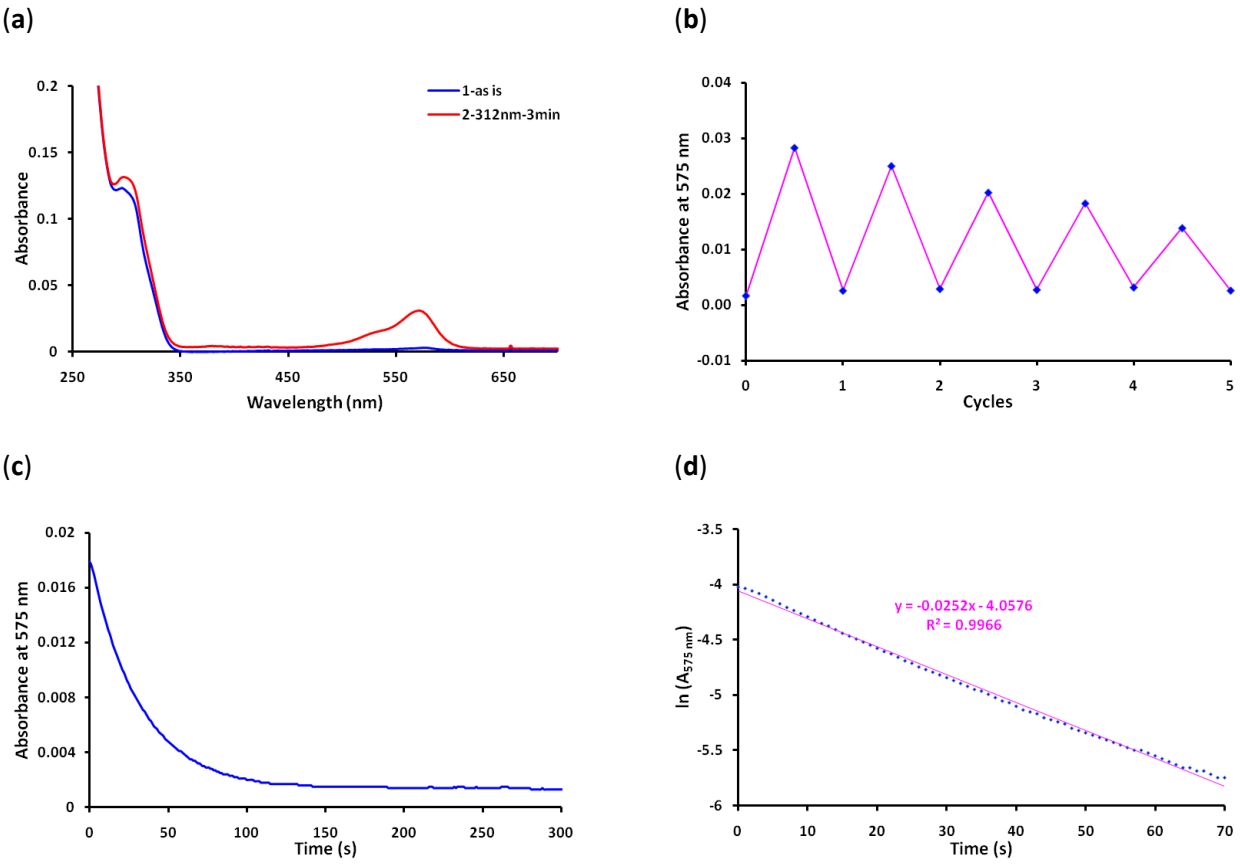

Figure S7. Opto-thermal switching properties of **1** (20 μM in 10 mM MOPS, 100 mM KCl, 1 mg/mL BSA, pH 7.2) in the presence of 100 mM Mg^{2+}: (**a**) absorbance spectra as dissolved in buffer solution and after irradiation with 312 nm light for 3 min; (**b**) absorbance changes at 575 nm in five cycles of UV irradiation (312 nm, 3 min) followed by thermal ring-closure in the dark; (**c**) time course for thermal ring-closure in the dark at 20 ^{o}C; (**d**) first-order rate plot for the thermal ring-closure.

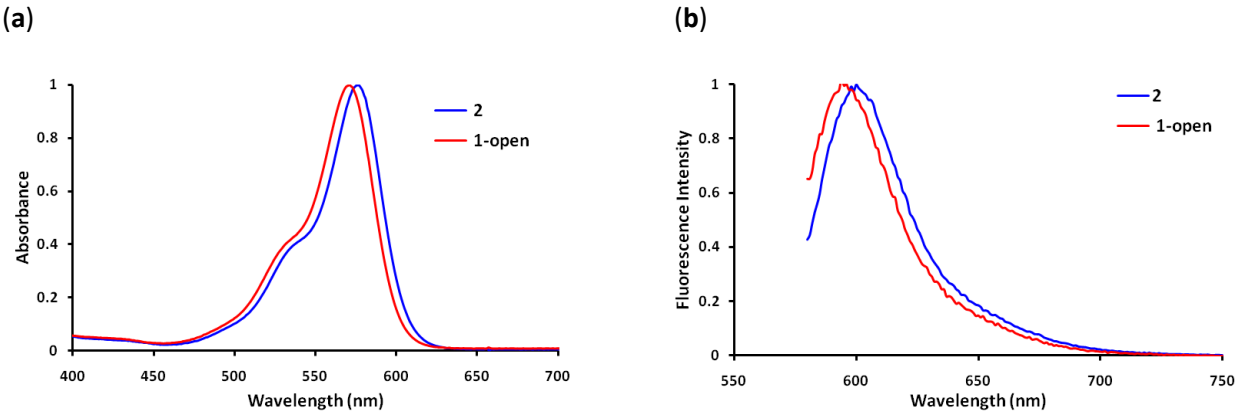

Figure S8. Normalized (**a**) absorbance and (**b**) fluorescence spectra (λ_{ex}=575 nm) for compound **2** and compound **1-open** (10 mM MOPS, 100 mM KCl, 1 mg/mL BSA, pH 7.20).

Copies of ^{1}H NMR, ^{13}C NMR and MS Spectra:

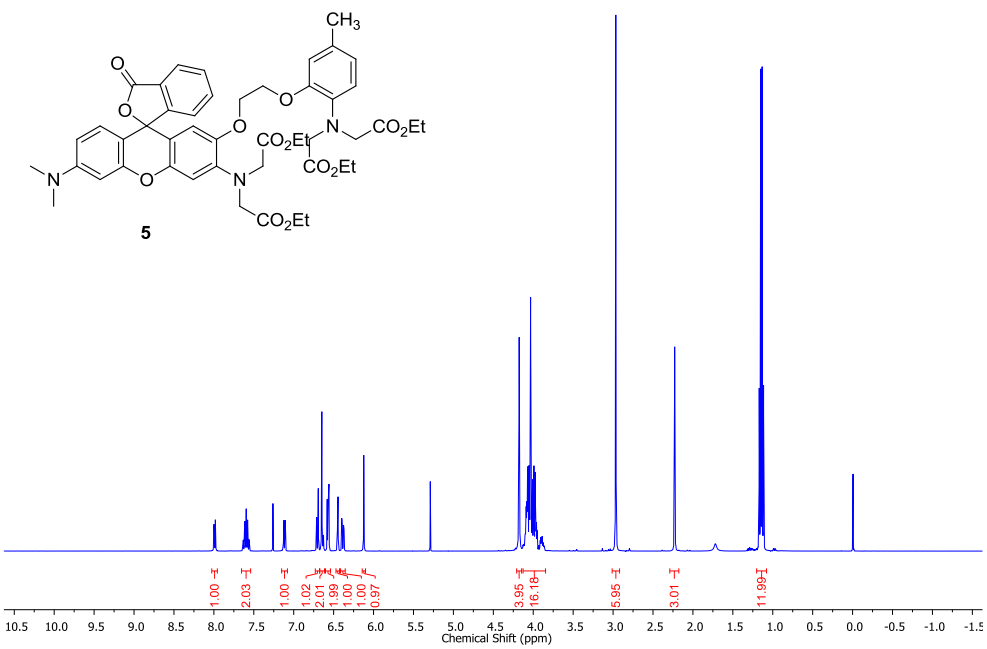

^{1}H NMR (400 MHz, $CDCl_3$) of compound **5**

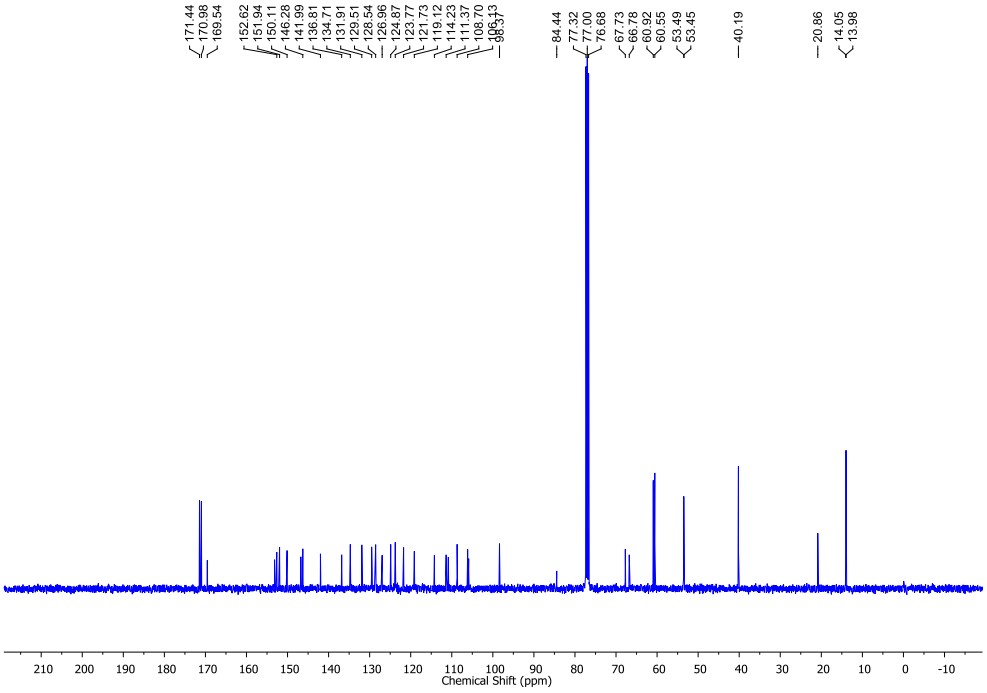

^{13}C NMR (100 MHz, $CDCl_3$) of compound **5**

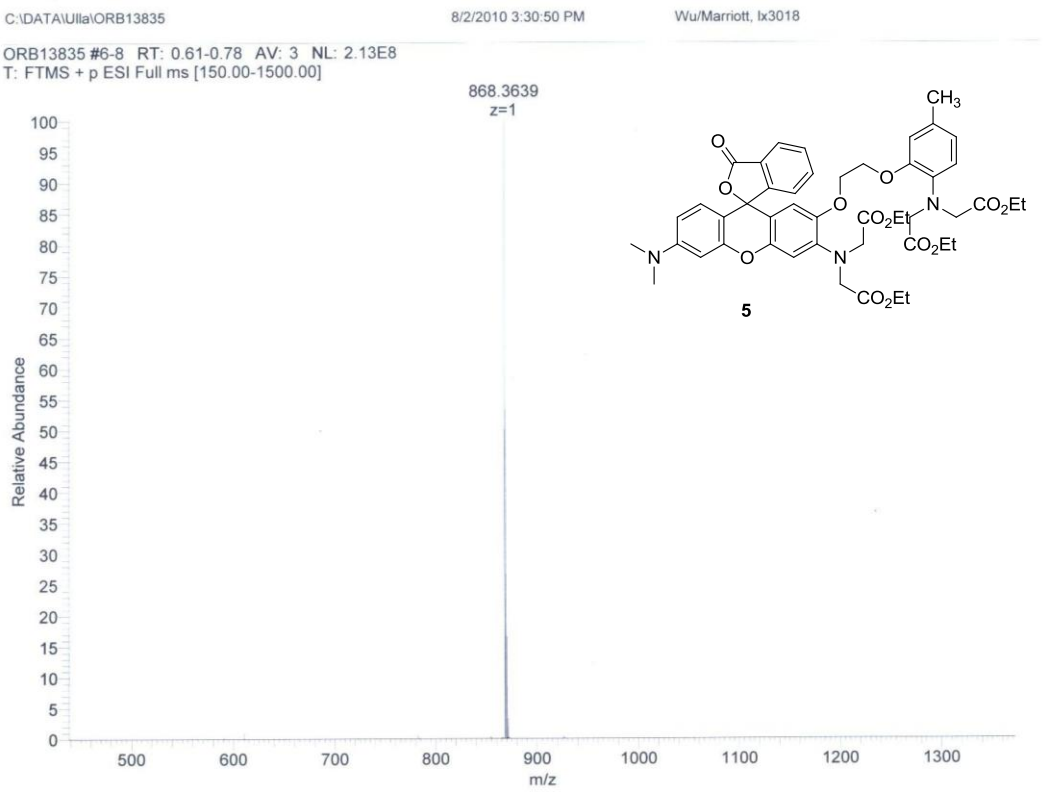

HRMS (ESI) of compound **5**

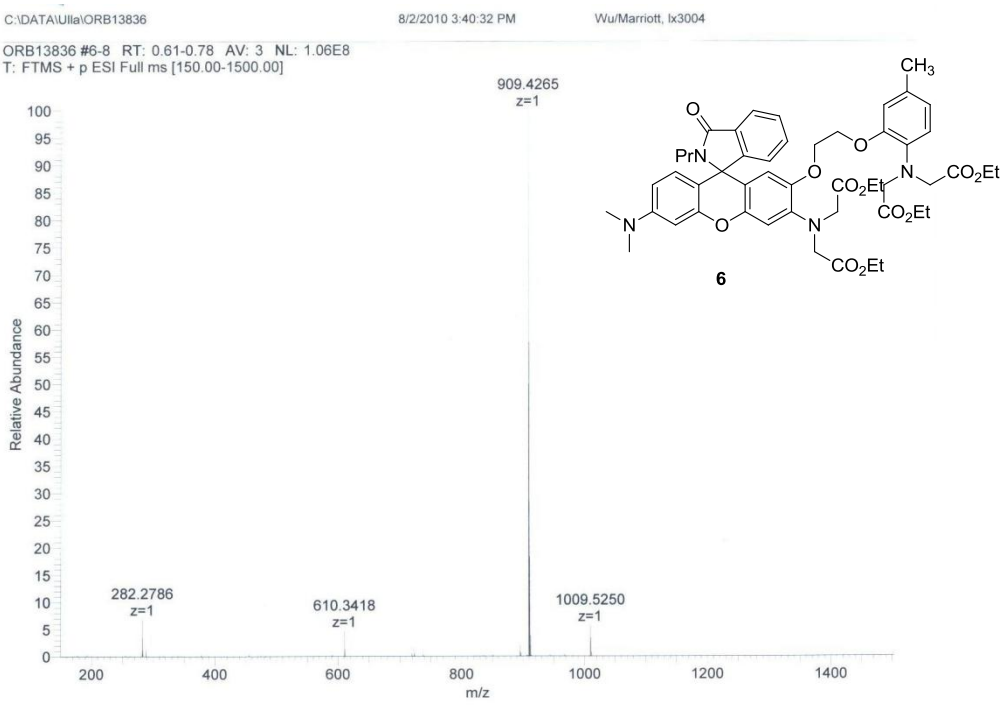

HRMS (ESI) of compound **6**

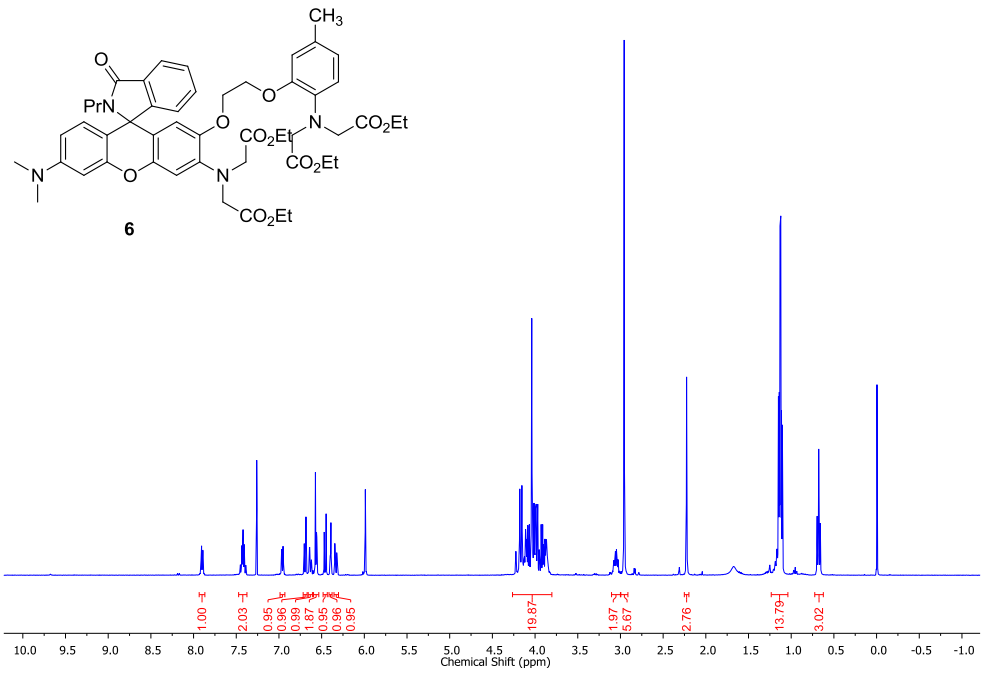

^{1}H NMR (400 MHz, $CDCl_3$) of compound **6**

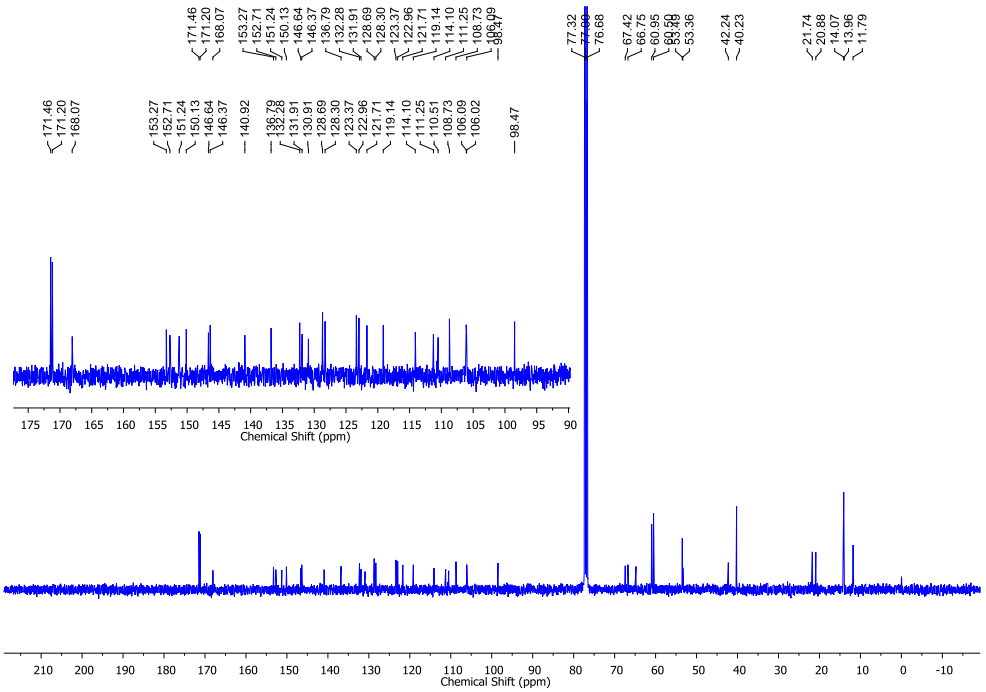

^{13}C NMR (100 MHz, $CDCl_3$) of compound **6**

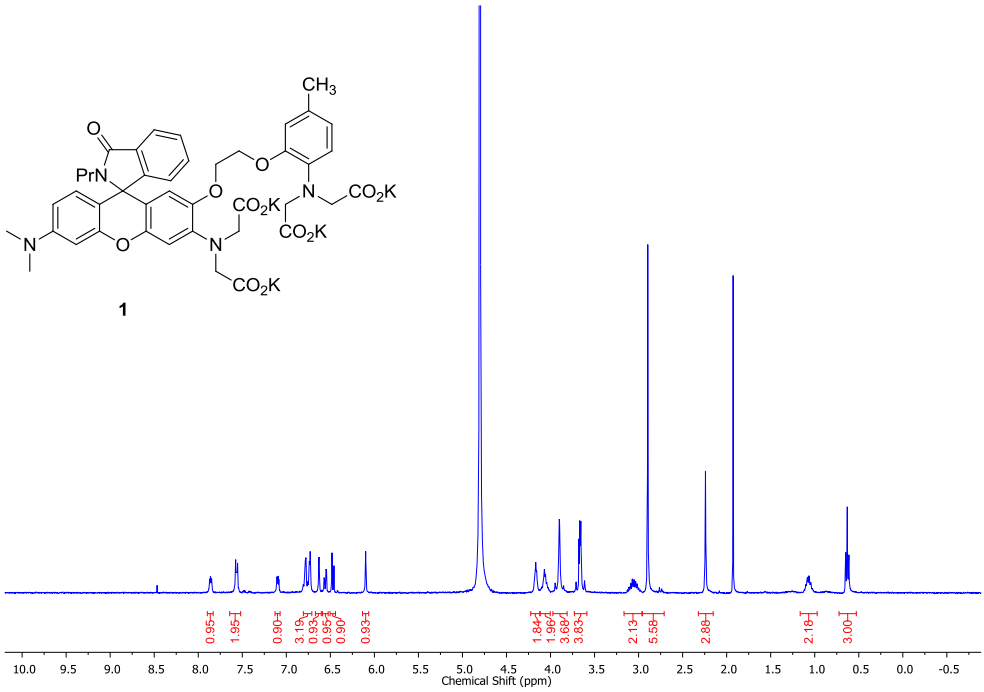

^{1}H NMR (400 MHz, D_2O) of compound **1**

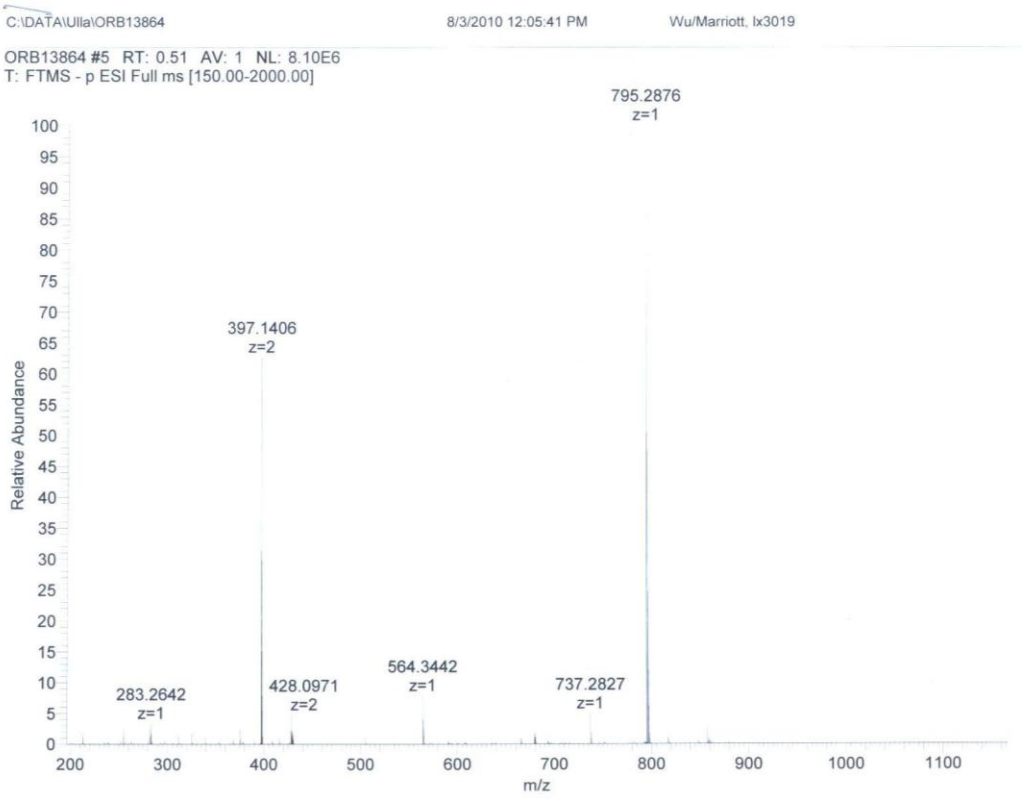

HRMS (ESI) of compound **1**

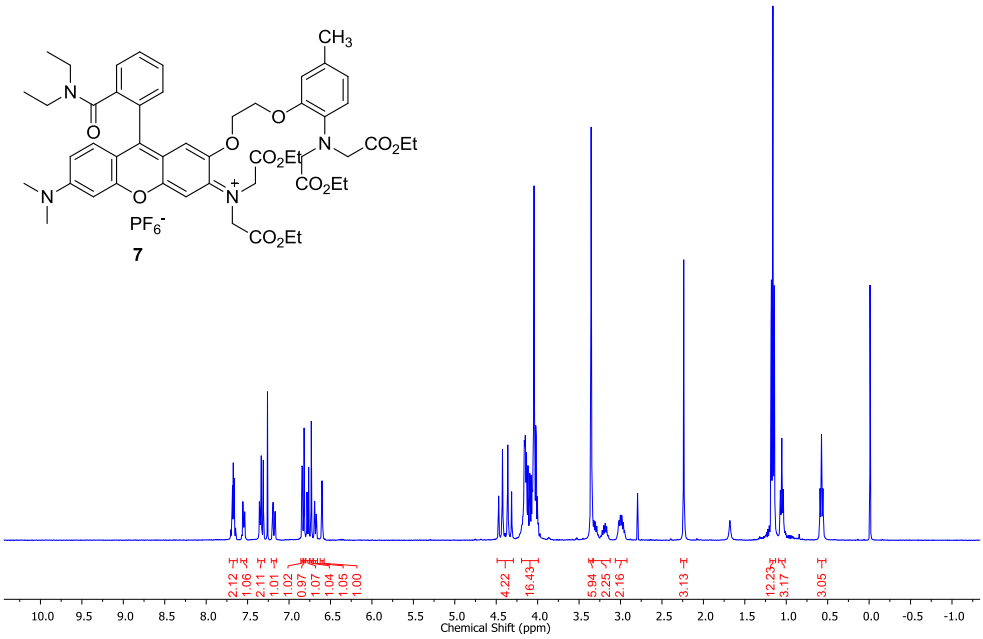

^{1}H NMR (400 MHz, $CDCl_3$) of compound **7**

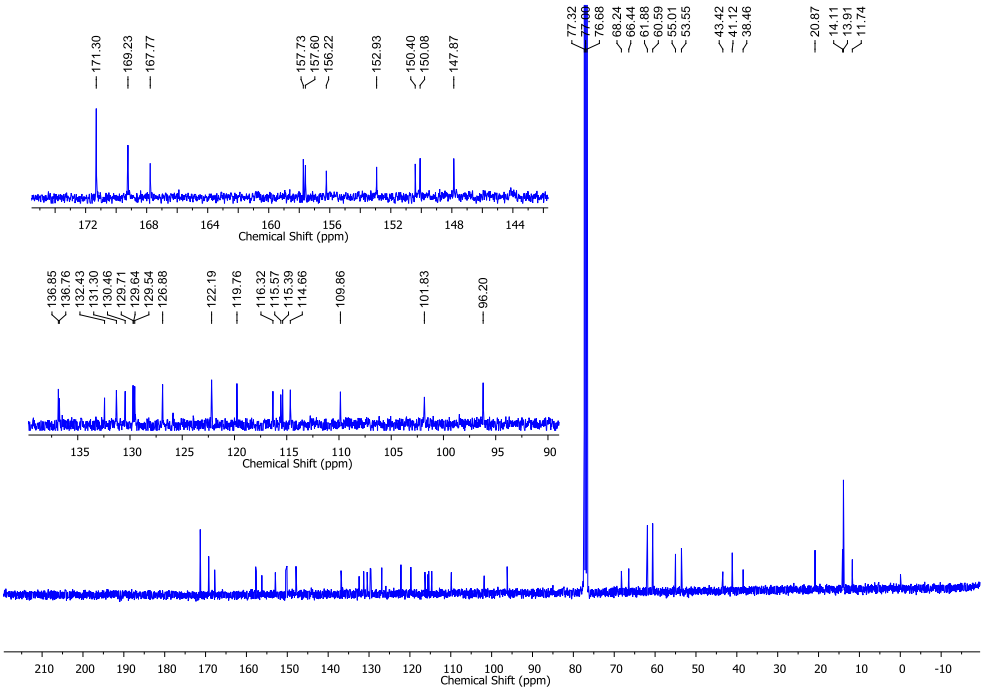

^{13}C NMR (100 MHz, $CDCl_3$) of compound **7**

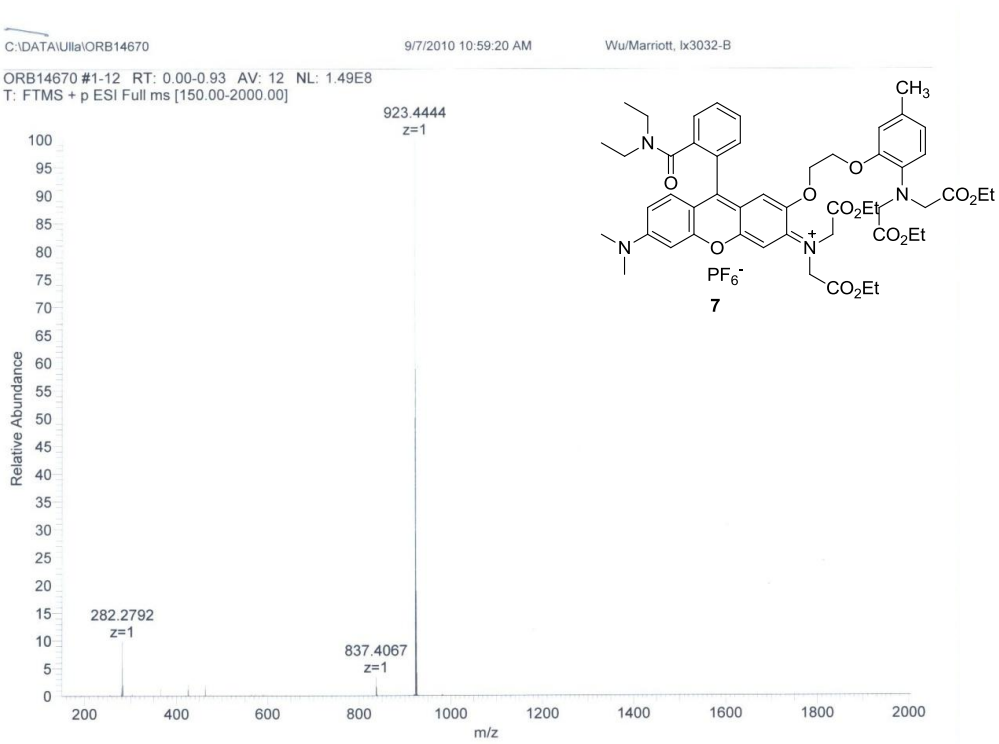

HRMS (ESI) of compound **7**

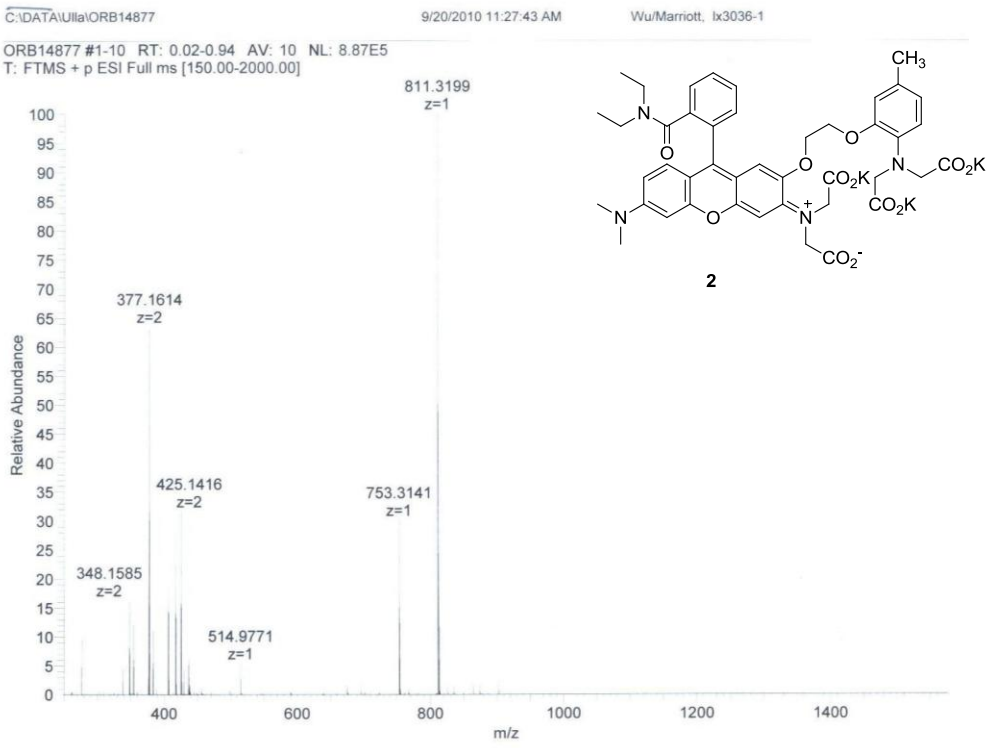

HRMS (ESI) of compound **2**

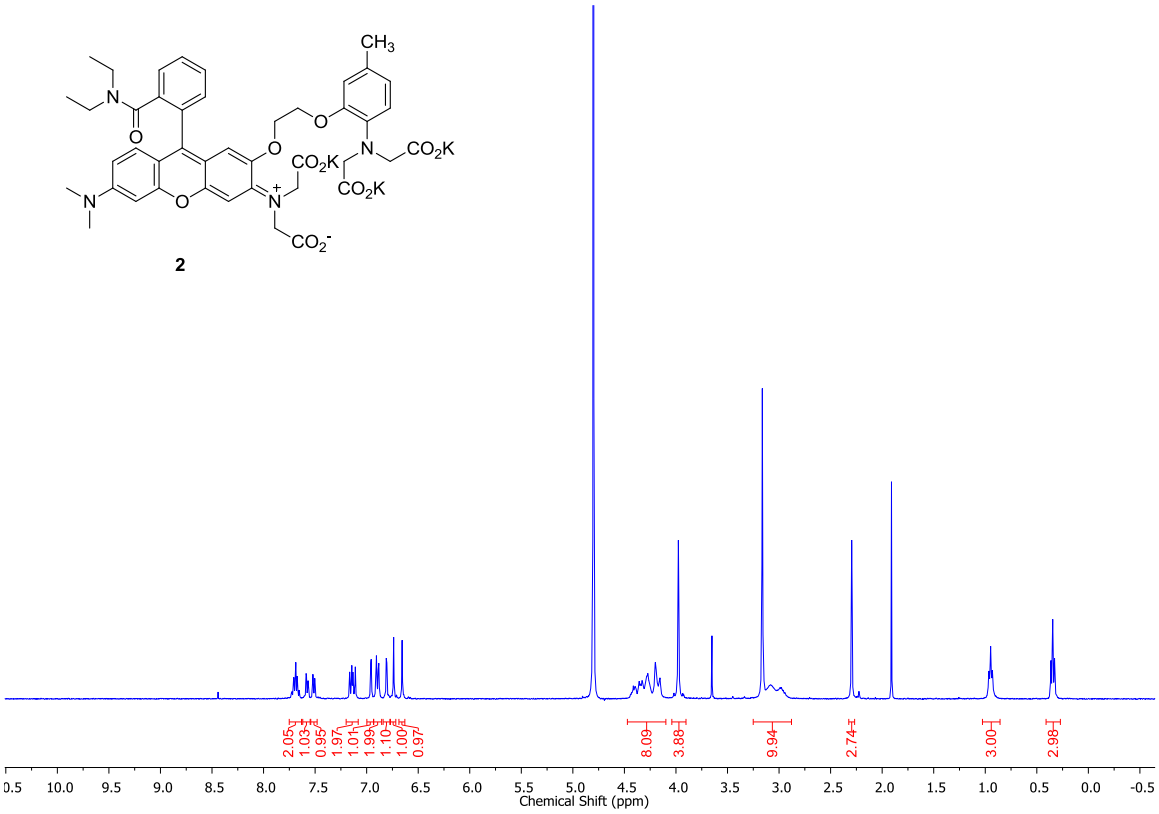

^{1}H NMR (400 MHz, D_2O) of compound **2**